JOURNAL OF AIRCRAFT
Vol. 47, No. 3, May–June 2010

Characterization of Aerospace Vehicle Performance and Mission Analysis Using Thermodynamic Availability

David W. Riggins*
Missouri University of Science and Technology, Rolla, Missouri, 65409
and
David J. Moorhouse† and Jose A. Camberos‡
Air Force Research Laboratory, Wright–Patterson Air Force Base, Ohio, 45433

DOI: 10.2514/1.46420

The fundamental relationship between entropy and aerospace vehicle and mission performance is analyzed in terms of the general availability rate balance between force-based vehicle performance, available energy associated with expended propellant, and the overall loss rate of availability, including the vehicle wake. The availability relationship for a vehicle is analytically combined with the vehicle equations of motion; this combination yields the balance between on-board energy rate usage and rates of changes in kinetic and potential energies of the vehicle and overall rate of entropy production. This result is then integrated over time for a general aerospace mission; as examples, simplified single-stage-to-orbit rocket-powered and air-breathing missions are analyzed. Examination of rate of availability loss for the general case of an accelerating, climbing aerospace vehicle provides a powerful loss superposition principle in terms of the separate evaluation and combination of loss rates for the same vehicle in cruise, acceleration, and climb. Rate of availability losses is also examined in terms of separable losses associated with the propulsion system and external aerodynamics. These loss terms are cast in terms of conventional parameters such as drag coefficient and engine specific impulse. Finally, rate losses in availability for classes of vehicles are described.

Nomenclature

A_{frontal}	=	frontal cross-sectional area of vehicle, m^2
a_{veh}	=	instantaneous acceleration of vehicle (linear), m/s^2
β	=	loss rate of availability per unit mass of vehicle, W/kg
C_D	=	vehicle drag coefficient based on A_{frontal}
$C_{P(P)}$	=	specific heat at constant pressure of propellant, J/kg K
D	=	external drag of vehicle, N
f	=	final mission state
f	=	fuel/air ratio for propulsion system (stoich denotes stoichimetric)
$F_{x(\text{engine})}$	=	net axial force on engine wetted surfaces, propulsion system = thrust, N
$F_{x(\text{flight})}$	=	overall (net) fluid-dynamic force component on vehicle in direction of flight, N
g, g_0	=	gravitational acceleration at altitude, sea level, m/s^2
h	=	altitude, m
$h_{i,l}$	=	static enthalpy per mass of species l on inflow to global control volume, J/kg K
$H_{o(P)}$	=	reference enthalpy of propellant at T_{ref}
H_P	=	heating value of propellant, J/kg
I_{sp}	=	engine specific impulse, s
L	=	vehicle lift, N
M	=	flight Mach number
$\dot{m}_i$	=	mass flow rate at entrance of global stream-tube (Fig. 1), kg/s
$\dot{m}_P$	=	propellant mass flow rate, kg/s
m_{veh}	=	vehicle mass, kg
$\dot{m}_w$	=	mass flow rate at exit of global stream-tube (Fig. 1), kg/s
NS	=	number of chemical species considered
P_i	=	ambient pressure, N/m^2
$\dot{Q}_{\text{flow-path}}$, $\dot{W}_{\text{flow-path}}$	=	heat and work rate interaction to main flowpath (excluding propellant subsystem) from vehicle, W
T	=	temperature, K
T_i	=	ambient temperature, K
$\dot{S}$	=	entropy rate, W/K
$\dot{S}_{\text{irr(total)}}$	=	total entropy rate due to irreversibility and nonideal heat transfer (vehicle and wake), W/K
s_l	=	entropy per mass of species l, J/kg K
T	=	temperature, K
T_i	=	ambient temperature, K
u_i, V	=	freestream velocity, vehicle flight velocity, m/s
$\mathbf{V}_{\text{inj}}$	=	propellant injection velocity vector, m/s
W	=	vehicle weight, N
$\alpha_{l,i}$, $\eta_{l,i}$	=	species mass and mole fractions of species at entrance i of global stream-tube (Fig. 1)
$\alpha_{l,w}$, $\eta_{l,w}$	=	species mass and mole fractions of species at exit w of global stream-tube (Fig. 1)
η	=	second-law effectiveness
θ	=	climb angle
λ	=	vehicle mass fraction

Received 20 July 2009; revision received 18 March 2010; accepted for publication 18 March 2010.

*Professor of Aerospace Engineering. Senior Member AIAA.
†Senior Scientist (Retired Emeritus), Air Vehicles Directorate. Associate Fellow AIAA.
‡Assistant to the Chief Scientist, Air Vehicles Directorate. Associate Fellow AIAA.

I. Introduction

LOSSES in thermodynamic availability are directly proportional to the generation of entropy associated with irreversible and nonideal processes occurring in an engineering system. Entropy (or thermodynamic availability losses) thus provides the common and consistent thermodynamic metric for loss analysis, loss minimization and optimization for all processes and subsystems within that system [1]. Although availability analysis is a fundamental and well-established approach for describing and quantifying losses in

ground-based systems of all types, it has not been widely used in the design, analysis and optimization of aerospace vehicles [2]. This has been due mainly to the lack of a sufficiently broad theoretical foundation which directly and unambiguously related availability and availability losses to classical (practical) measures of vehicle performance and performance losses, specifically within a concise availability-performance balance equation. Nevertheless, early seminal work done in this area includes that of Oswatitsch [3] who first derived the availability rate balance for a nonpowered aerodynamic shape in flight; this work directly related the aerodynamic drag to availability losses (entropy generation) in the flow-field, including in the wake. This availability rate balance has been now been extended by Giles and Cummings [4] and Hunt et al. [5] to powered vehicles with simple energy addition. They noted the importance of the net overall fluid-dynamic force component experienced by all vehicle surfaces in the direction of vehicle movement within that balance. Riggins et al. [6] more recently provided the availability rate balance for a general aerospace vehicle with propellant mass and energy addition and chemical reaction. The main objective of the current paper is to provide a detailed analytical examination of the general characteristics of this governing availability rate balance for general aerospace vehicles in terms of flight regimes and broad vehicle types. In addition, the availability balance is analytically combined with the aerospace vehicle equations of motion; this allows time-integration across vehicle missions and therefore provides the fundamental overall governing balance between total input energy, mission-integrated vehicle performance, and cumulative losses.

The design and characteristics of an atmospheric flight vehicle are generally determined by the broad requirement to drive the vehicle through the air in order to translate the vehicle and an associated payload from one point to another. Although the traditional concepts of drag and thrust (and lift and side-forces) provide the default force definition framework in vehicle design and evaluation, it is the single net fluid-dynamic force vector on all wetted surfaces of the vehicle including the fuel/propellant systems and associated tanks along with the vehicle weight vector that determines the vehicle flight characteristics, i.e., where the vehicle goes and how long it takes to get there, etc. The definitions of lift, drag, and thrust are simply agreed-upon and convenient components of that overall resultant force vector. In the case of high-speed engine thrust or other defined engine component forces, the separate distinction made between aerodynamic and propulsive domains is especially arbitrary, since the exact orientation and scope of those engine thrust force components depends entirely on the discretion of the engineer, i.e., specific force accounting definitions used (i.e. where does the engine begin and end in terms of wetted surfaces and what is the line defining the engine thrust force action?) Hence, it is especially useful to properly consider an aerospace vehicle as a single and continuous wrapped or closed wetted surface over which differential pressure and shear forces act, with no fundamental or primary distinctions made in terms of components or the separation of discrete subsystems of aerodynamics and propulsive flowpaths.

With this last observation, the fundamental importance of that specific component of the overall fluid-dynamic force vector which lies in the direction of instantaneous vehicle movement for an atmospheric flight vehicle is then obvious in terms of providing the framework for describing losses and work/energy characteristics of the vehicle as a whole. In this paper, this component will generally be designated as the net axial force in the sense that the local direction of vehicle movement at the moment of interest coincides with the instantaneous x axis. Note that both vehicle power requirements and loss characteristics associated with the generation of out-of-axial aerodynamic forces, i.e., lift and side-forces, are included in this observation. This is because all vehicle power requirements and realized losses including the inarguable power requirements and losses associated with lift generation ultimately must cascade back to and contribute to the resultant power requirements and losses associated with the sheer necessity of driving the vehicle and its payload through the fluid medium. The proper allocation/quantification of losses and power requirements can then in fact explicitly include the effects of lift and side-force generation; this allocation is, however, done through detailed consideration of the inevitable impact of these losses on the net fluid-dynamic force component aligned with vehicle movement and ultimately on the entropy production within the flow and entropy transfer to the flow.

In this paper, overall on-board energy usage is derived in terms of vehicle kinetic and potential energy changes and the overall mission-integrated loss in availability (described in terms of the universal metric of entropy generation). This methodology is applied to simplified single-stage-to-orbit (SSTO) mission configurations for both rocket-powered and air-breathing vehicles in order to clarify second-law issues involving the feasibility and comparison of such missions. Loss rates of availability for vehicles are then examined in terms of conventional performance information such as drag coefficient, engine specific impulse, sizing, etc. This allows the quantitative evaluation of loss rates for various classes and types of vehicles and for the entire spectrum of velocity-altitude describing flight, with specific implementation here of simple models for rockets and air-breathing vehicles.

Early work done in the area of entropy and availability-based assessment of aerospace jet engine performance includes that of Foa [7] and Builder [8]. Foa sketched the characterization of performance system thrust and propulsive losses in terms of entropy rise across a jet engine. The entropy method was defined with matched pressure across the engine and other simplifying assumptions. This is similar to the more general work of Riggins [9] who examined the thermodynamic spectrum of gas turbine engine performance from the standpoint of overall heat added, irreversibility and work exchange in the propulsive flowpath. Lewis [10] provided clarification regarding the role of the second law in providing a universal definition of the propulsive efficiency for an isolated engine. The concept of thrust or thrust-work potential (also called stream-thrust based methods) for the performance characterization of high-speed ramjet and scramjet engines were first articulated by Curran and Craig [11]; considerable extension of their seminal work has been performed by Riggins et al. [12,13]. The use of these methods has enabled the complete characterization of the loss in scramjet engine thrust due to irreversibility and has allowed the assessment of engine thrust losses in terms of irreversible loss mechanism and location. In a closely related development, the general concept of work availability as applied to aerospace jet turbine engines has been developed and used by Roth [14,15] who suggested the use of work availability as a common currency for engine design, evaluation, and optimization, generally without explicit second-law considerations. In addition, a significant amount of work has also been done in the area of applying conventional availability (alternatively termed exergy) to the problem of aerospace engine and engine component analysis and design. Such work includes that by Clarke and Horlock [16] and Czysz and Murthy [17]. However, Riggins [18,19] has shown problems with conventional availability when directly applied to very simple isolated jet engine optimization problems and has suggested a modification which unifies it with the stream-thrust concepts discussed above.

The references listed above which describe some of the previous/related work in the area of performance assessment using entropy and availability (or exergy) are specific to propulsion systems for flight vehicles. There has been significantly less work involving the development and use of entropy-based methods for external aerodynamic design, evaluation and optimization, or (especially) for overall vehicles. In addition to past work involving specific overall availability balances for aerospace vehicles which has been described previously in this section as particularly relevant to the current paper (i.e. [3–6]), Greene [20] examined the role of entropy for induced drag minimization on low-speed airfoils using concepts related to this earlier work. Roth [21] and Roth and Mavris [22] have usefully extended work potential methods to a vehicle airframe with a turbine engine propulsion system and overall vehicle system loss management. Riggins et al. [23] discuss the necessity and methodology for evaluating and including the coupled wake availability losses associated with corresponding upstream (vehicle) availability losses, when using availability analysis for aerospace vehicles.

II. Availability Balance for Aerospace Vehicles: Background

The relationship between the overall net aero/propulsive fluid-dynamic force in the direction of aerospace vehicle movement and entropy production and energy effects has been derived and discussed in [6]; see the development in this earlier work for notation and definitions. This availability rate balance is derived from fundamental energy and entropy considerations applied to the global or overall control volume as sketched in Fig. 1 encompassing an aerospace vehicle and its surroundings (including the wake region). The global stream-tube must be made large enough in span (i.e. in terms of the plane perpendicular to vehicle movement) in order to realize the asymptotic limit inherent in the wake mixing process itself, for accurate analytical computation of the wake entropy generation. However, there is no necessity to define an axial length scale for the wake region since the wake entropy generation computation is defined by a simple single-step flow rate based analytical procedure between stations e and w [6].

The powerful availability rate relationship which results for the general case of an aerospace vehicle in flight with propellant addition to the global stream-tube between stations i and e is written as

$$\begin{aligned} F_{x(\text{flight})} \cdot u_i &= \dot{Q}_{\text{flow-path}} + \dot{W}_{\text{flow-path}} + \dot{m}_p \frac{u_i^2}{2} \\ &+ \dot{m}_p \frac{\mathbf{V}_{\text{inj}} \cdot \mathbf{V}_{\text{inj}}}{2} + \dot{m}_p \left\{ h_{0(P)} + \int_{T_{\text{ref}}}^{T_{\text{inj}}} C_{p(P)}\, \mathrm{d}T \right\} \\ &- \dot{m}_w \sum_{l=1}^{\text{NS}} \alpha_{l,w} [h_{i,l} - T_i s_l(T_i, P_i, \eta_{l,w})] \\ &+ \dot{m}_i \sum_{l=1}^{\text{NS}} \alpha_{li} [h_{i,l} - T_i s_l(T_i, P_i, \eta_{l,i})] \\ &- T_i (\dot{S}_{\text{vehicle}} + \dot{S}_{\text{wake}} + \dot{S}_{\text{inj}}) \end{aligned} \tag{1}$$

In this equation, u_i is the magnitude of the flight velocity of the vehicle. The left-hand side represents the vehicle (net) axial force-power (in the direction of vehicle movement). Specifically, $F_{x(\text{flight})}$ is the net axial component of the overall force vector due to all pressure and shear forces on all vehicle wetted surfaces, including fuel systems/tanks, external aerodynamics, and propulsive flowpath(s). The first and second term on the right-hand side represent the overall (net) energy rates added as heat and work interactions from the vehicle into the flowpath(s) associated with the global stream-tube (but not including the fuel system); the third term represents the kinetic energy rate associated with the injected propellant; the fourth and fifth term represent inclusively the total enthalpy rate associated with propellant injection (designated by the subscript inj); while the sixth and seventh term represent the change in chemical potential across the global stream-tube from inlet (i) to equilibrated wake exit plane (w). Finally, the last (eighth) term on the right-hand side of Eq. (1) is the availability loss rate associated with 1) all entropy (irreversible) generation or entropy transferred from the vehicle in and around the vehicle (from station i to station e) ($\dot{S}_{\text{vehicle}}$), 2) entropy generation in the unconstrained wake process (from station e to station w) ($\dot{S}_{\text{wake}}$), and 3) the entropy flow rate associated with the injected propellant ($\dot{S}_{\text{inj}}$). It should be noted that $\dot{S}_{\text{vehicle}}$ in this equation excludes any entropy generation or transfer within or to the fuel system (which is accounted for through $\dot{S}_{\text{inj}}$).

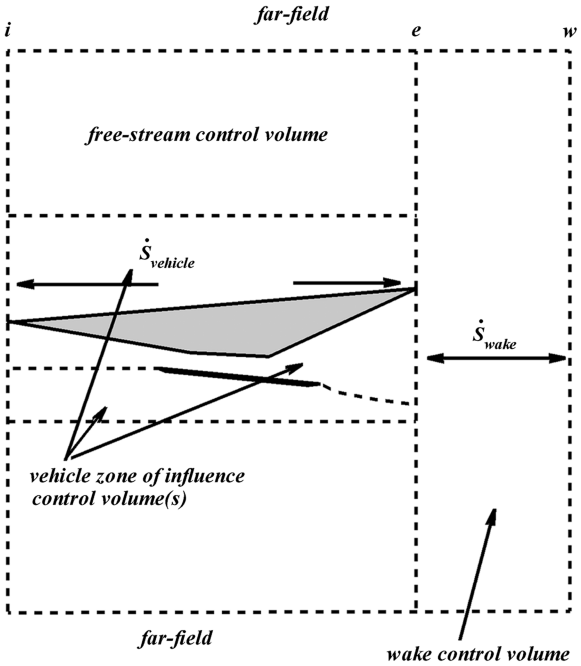

Fig. 1 Global stream-tube for entropy-performance relationship [for use in Eq. (1–4)].

For the case of a thermally balanced vehicle with propellant tank (reservoir) conditions designated as tanks, this expression is rewritten as

$$F_{x(\text{flight})} \cdot u_i = \dot{m}_p \left(H^* + \frac{u_i^2}{2} \right) - T_i (\dot{S}_{\text{irr-vehicle}} + \dot{S}_{\text{wake}}) \tag{2}$$

where

$$\begin{aligned} \dot{m}_p H^* &= \dot{m}_p \left\{ h_{0(p)} + \int_{T_{\text{ref}}}^{T_{\text{tanks}}} C_{p(p)}\, \mathrm{d}T \right\} - T_i \dot{S}_{\text{tanks}} \\ &- \dot{m}_w \sum_{l=1}^{\text{NS}} \alpha_{lw} [h_{il} - T_i s_l(T_i, P_i, \eta_{lw})] \\ &+ \dot{m}_i \sum_{l=1}^{\text{NS}} \alpha_{li} [h_{il} - T_i s_l(T_i, P_i, \eta_{li})] \end{aligned} \tag{3}$$

In this relationship, $\dot{S}_{\text{irr-vehicle}}$ is now the total entropy generation rate from i to e in the global stream-tube due to all irreversibilities out to the exit plane of the vehicle, including aerodynamic, propulsive, and fuel subsystems. H^* is the change in the chemical potential from the freestream air and the propellant in tanks to the equilibrated wake outflow.

This relationship [Eq. (2)] can be represented using the following approximate formulation [1], where H_P is the heating value of the propellant:

$$F_{x(\text{flight})} u_i = \dot{m}_p \left[\frac{u_i^2}{2} + H_P \right] - T_i (\dot{S}_{\text{irr-vehicle}} + \dot{S}_{\text{wake}}) \tag{4}$$

This formulation in Eq. (4) represents a conservative approximation since H_P is typically somewhat less than H^* for reasonable propellant pressures and temperatures. Specifically, H_P can be shown to range from a few percent lower than H^* for H_2–air systems to over 10% lower than H^* for H_2-O_2 rockets, across a wide range of propellant conditions. Although this approximation is sufficient for the broad capabilities and analysis developed in subsequent sections of the present work, more detailed studies should incorporate the availability rate balances provided by Eq. (1) or Eq. (2).

III. Combination of Availability Balance with Vehicle Equations of Motion

This section provides the synthesis of the availability rate balance for a vehicle in Eq. (4) with the standard vehicle equations of motion. This synthesis produces powerful analytical relationships describing both vehicle and mission performance and optimization in terms of overall availability and availability losses.

Consider an aerospace vehicle in flight in the atmosphere (see Fig. 2 below) in which the x axis is aligned with the instantaneous direction of flight (i.e. the direction coincident with the incoming freestream velocity vector). For simplicity, consider the vehicle as

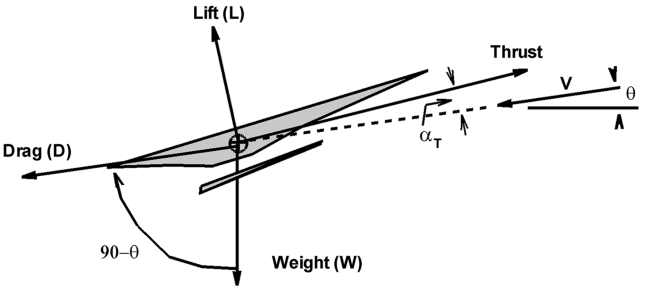

Fig. 2 Vehicle configuration for equations of motion analysis.

operating in the two-dimensional plane although that is not necessary in terms of the analysis. Also replace the notation u_i (freestream velocity) in Eq. (4) with V to designate the vehicle flight velocity.

Define the thrust as shown in Fig. 2 as the net force component along the defined engine axis due to all pressure and shear forces associated with the wetted surfaces of the propulsion system. The specific component of the thrust vector in the direction of vehicle movement (along the x axis) is designated $F_{x(\text{engine})}$. For the present work, small $\propto_T$ is assumed such that $F_{x(\text{engine})} =$ thrust. If $\propto_T$ is not zero, a portion of the engine thrust operates in a direction perpendicular to the x axis, i.e., will contribute to the lift force, L. The lift force L is defined here as the net force component perpendicular to the x direction due to all pressure and shear forces associated with all wetted surfaces of the vehicle, external and internal. The drag force D is the net force component due to all pressure and shear forces acting in the x direction not associated with the propulsion system. The climb angle θ is the angle between the flight path (relative wind) and the horizontal.

The instantaneous equation of motion in the flight direction for the vehicle with mass m_{veh} is as follows:

$$F_{x(\text{engine})} - D - m_{\text{veh}} g \sin\theta = m_{\text{veh}} \frac{\mathrm{d}V}{\mathrm{d}t} \tag{5}$$

The overall net fluid-dynamic force component experienced by the vehicle in the flight direction is $F_{x(\text{flight})}$ where

$$F_{x(\text{flight})} = F_{x(\text{engine})} - D \tag{6}$$

Hence,

$$F_{x(\text{flight})} = m_{\text{veh}} g \sin\theta + m_{\text{veh}} \frac{\mathrm{d}V}{\mathrm{d}t} \tag{7}$$

Write the instantaneous power associated with the work done by $F_{x(\text{flight})}$ as

$$F_{x(\text{flight})} V = m_{\text{veh}} V \frac{\mathrm{d}V}{\mathrm{d}t} + m_{\text{veh}} V g \sin\theta \tag{8}$$

Now, rewrite the availability balance (force–entropy) relationship [Eq. (4)] for a nominally thermally balanced aerospace vehicle:

$$F_{x(\text{flight})} V = \dot{m}_p \left[\frac{V^2}{2} + H_P\right] - T_i \dot{S}_{\text{irr(total)}} \tag{9}$$

Here H_P is the heating value of the fuel and $\dot{m}_p$ is the mass flow rate of propellant. $\dot{S}_{\text{irr(total)}}$ is the total entropy production rate associated with irreversibilities including the wake equilibrium process and nonideal heat transfer, i.e.,

$$\dot{S}_{\text{irr(total)}} = \dot{S}_{\text{irr(veh)}} + \dot{S}_{\text{wake}} \tag{10}$$

Equate these two expressions [Eqs. (8) and (9)] to obtain

$$\dot{m}_p \left[\frac{V^2}{2} + H_P\right] - T_i \dot{S}_{\text{irr(total)}} = m_{\text{veh}} V \frac{\mathrm{d}V}{\mathrm{d}t} + m_{\text{veh}} V g \sin\theta \tag{11}$$

Now $\dot{m}_p = -\mathrm{d}m_{\text{veh}}/\mathrm{d}t$ by definition so this expression can be written as

$$-\frac{\mathrm{d}m_{\text{veh}}}{\mathrm{d}t}\left[\frac{V^2}{2} + H_P\right] - T_i \dot{S}_{\text{irr(total)}} = m_{\text{veh}} V \frac{\mathrm{d}V}{\mathrm{d}t} + m_{\text{veh}} V g \sin\theta \tag{12}$$

Furthermore $V \sin\theta = \mathrm{d}h/\mathrm{d}t$ where $\mathrm{d}h$ is the differential change in altitude of the vehicle and $\dot{S}_{\text{irr(total)}} = \mathrm{d}S_{\text{irr(total)}}/\mathrm{d}t$ where $\mathrm{d}S_{\text{irr(total)}}$ is the entropy generation due to irreversibilities and nonideal heat transfer across both vehicle control volume and wake equilibration process during time $\mathrm{d}t$.

Therefore, the following is written:

$$-\mathrm{d}m_{\text{veh}}\left[\frac{V^2}{2} + H_P\right] - T_i \mathrm{d}S_{\text{irr(total)}} = m_{\text{veh}} V \mathrm{d}V + (m_{\text{veh}} g)\mathrm{d}h \tag{13}$$

By definition, $V\mathrm{d}V = \mathrm{d}(V^2/2)$. Therefore,

$$-T_i \mathrm{d}S_{\text{irr(total)}} = dm_{\text{veh}}\left[\frac{V^2}{2} + H_P\right] + m_{\text{veh}}\mathrm{d}\left[\frac{V^2}{2}\right] + (m_{\text{veh}} g)\mathrm{d}h \tag{14}$$

Now note that since the heating value of the propellant H_P is fixed

$$\mathrm{d}\left[\frac{V^2}{2}\right] = \mathrm{d}\left[\frac{V^2}{2} + H_P\right] \tag{15}$$

Therefore,

$$-T_i dS_{\text{irr(total)}} = dm_{\text{veh}}\left[\frac{V^2}{2} + H_P\right] + m_{\text{veh}}\mathrm{d}\left[\frac{V^2}{2} + H_P\right] + (m_{\text{veh}} g)\mathrm{d}h \tag{16}$$

This can be then written using the chain rule of differentiation as

$$-T_i \mathrm{d}S_{\text{irr(total)}} = \mathrm{d}\left[m_{\text{veh}} \frac{V^2}{2} + m_{\text{veh}} H_P\right] + (m_{\text{veh}} g)\mathrm{d}h \tag{17}$$

This can be rearranged and integrated across a mission as follows:

$$H_P \Delta(\text{propellant mass used}) - \int_{\text{mission}} T_i \, \mathrm{d}S_{\text{irr(total)}} = \Delta\left(m_{\text{veh}} \frac{V^2}{2}\right) + \int_{\text{mission}} m_{\text{veh}} g \, \mathrm{d}h \tag{18}$$

In this important balance equation:

1) $\Delta(m_{\text{veh}} \frac{V^2}{2})$ is the change in vehicle kinetic energy across the mission.

2) $\int_{\text{mission}} m_{\text{veh}} g \, \mathrm{d}h$ is the change in vehicle gravitational potential energy across the mission.

3) $H_P \Delta$(propellant mass used) is the energy content associated with the expended propellant across the mission.

4) $\int_{\text{mission}} T_i \, \mathrm{d}S_{\text{irr(total)}}$ ($= T_i \Delta S_{\text{irr(total)}}$ for assumption of constant T_i) is the cumulative availability loss associated with all irreversibilities occurring during the mission including in the wake of the vehicle.

It should be noted that Eqs. (1–4) which describe the availability rate balance for an aerospace vehicle in flight at velocity V, are formally derived in [6] using the assumption of steady flow throughout the global control volume. Therefore, when integrating across time as done here, it is assumed that the time and amplitude scale of dynamic events (such as those associated with vehicle accelerations) are not sufficient to significantly affect that availability balance at any given time of interest. Note, however, that Eq. (18) is exact in all cases for defined missions with steady state initial and end states.

A generic sketch showing the fractions of overall on-board energy used in a mission is given in Fig. 3. The overall quantity of heat-release energy associated with propellant mass used during the mission is subdivided using Eq. (18) into three main categories corresponding to vehicle kinetic energy change, vehicle altitude

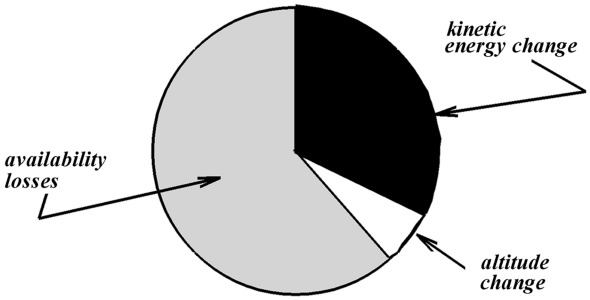

Fig. 3 Sketch of typical on-board energy usage from Eq. (16) (fractions of overall on-board energy used in a mission).

change, and losses in total availability. Either or both of the kinetic energy and the altitude (potential energy) terms can be negative across a mission; the loss term is always positive, of course.

This relationship can be used to define a mission-based availability metric which essentially provides the common currency (through the $S_{\text{irr(total)}}$) for vehicle loss assessment and optimization across a mission:

$$Ex_{\text{veh,mission}} = H_P \Delta(\text{propellant mass used}) - \int_{\text{mission}} T_i \, \mathrm{d}S_{\text{irr(total)}} \tag{19}$$

Maximizing this parameter maximizes (optimizes) the sum of the kinetic energy and potential energy changes for a given mission. A mission-based efficiency for a powered vehicle is also directly defined as

$$\eta_{\text{mission}} = \frac{H_P \Delta(\text{propellant mass used}) - \int_{\text{mission}} T_i \, \mathrm{d}S_{\text{irr(total)}}}{H_P \Delta(\text{propellant mass used})} \tag{20}$$

or

$$\eta_{\text{mission}} = 1 - \frac{\int_{\text{mission}} T_i \, \mathrm{d}S_{\text{irr(total)}}}{H_P \Delta(\text{propellant mass used})} \tag{21}$$

One can also define an instantaneous measure of second-law powered-vehicle effectiveness by defining

$$\eta = 1 - \frac{T_i \dot{S}_{\text{irr(total)}}}{H_P \dot{m}_p} \tag{22}$$

where $\dot{m}_p$ is the instantaneous mass flow rate of propellant expended by the vehicle. This implies that one always wants to minimize the entropy generated due to irreversibility per kilogram of propellant expended.

Note that the limiting case of a vehicle in cruise simply implies that

$$\left(H_P + \frac{V^2}{2}\right) \Delta(\text{propellant mass used}) = \int_{\text{mission}} T_i \, \mathrm{d}S_{\text{irr(total)}} \tag{23}$$

Therefore, for a vehicle in cruise, minimum propellant usage simply corresponds to minimum overall (vehicle and wake) entropy production.

For the limiting case of a vehicle with no propellant usage, the goal would also correspond to the minimization of overall (vehicle and wake) entropy production, at least for realizing the smallest losses in altitude and/or velocity.

It is emphasized once again that the entropy generation term that appears in these relationships must include the wake entropy generation.

IV. Propellant Mass Fraction Analysis

The following section examines the propellant mass fraction characteristics which result from examination and analysis of Eq. (18).

The vehicle (overall) propellant mass fraction is defined as follows:

$$\lambda_P = \frac{\Delta(\text{propellant mass used})}{m_{\text{veh(initial)}}} \tag{24}$$

In this expression $m_{\text{veh(initial)}}$ is the initial vehicle mass at the beginning of a mission. This quantity can be defined using Eq. (18) as follows:

$$\lambda_P = \frac{\Delta(m_{\text{veh}} \frac{V^2}{2})}{H_P m_{\text{veh(initial)}}} + \frac{\int_{\text{mission}} m_{\text{veh}} g \, \mathrm{d}h}{H_P m_{\text{veh(initial)}}} + \frac{\int_{\text{mission}} T_i \, \mathrm{d}S_{\text{irr(total)}}}{H_P m_{\text{veh(initial)}}} \tag{25}$$

or

$$\lambda_P = \lambda_{P,\text{KE}} + \lambda_{P,\text{PE}} + \lambda_{P,\text{LOSS}} \tag{26}$$

Here,

$$\lambda_{P,\text{KE}} = \frac{\Delta(m_{\text{veh}} \frac{V^2}{2})}{H_P m_{\text{veh(initial)}}} \tag{27}$$

$$\lambda_{P,\text{PE}} = \frac{\int_{\text{mission}} m_{\text{veh}} g \, \mathrm{d}h}{H_P m_{\text{veh(initial)}}} \tag{28}$$

$$\lambda_{P,\text{LOSS}} = \frac{\int_{\text{mission}} T_i \, \mathrm{d}S_{\text{irr(total)}}}{H_P m_{\text{veh(initial)}}} \tag{29}$$

The first term on the right-hand side of this expression, $\lambda_{P,\text{KE}}$ represents the propellant mass fraction associated with the kinetic energy change of the vehicle across the mission. The second term on the right-hand side $\lambda_{P,\text{PE}}$ represents the propellant mass fraction associated with the potential energy change across the mission. The last term, $\lambda_{P,\text{LOSS}}$ represents the propellant mass fraction available and necessary for overcoming losses (irreversibilities) of all types during the mission.

It is important to realize that the kinetic energy and the potential energy terms can be negative in this thermodynamically consistent formulation, for either a segment of a mission or over the entire mission. However, the analysis mandates that the loss term must be (and is) always positive and increases with time throughout a mission. Further the required cumulative overall propellant mass fraction (in terms of propellant used) always increases (or, at best, stays the same) with time throughout a mission. For instance, consider a power-off deceleration (no propellant used, zero or negative thrust). In such a situation, the kinetic energy propellant mass fraction would by definition be negative. This is true whether that power-off deceleration maneuver was accomplished by increasing altitude, or by simply decelerating via aerodynamic drag, or through a combination of the two effects. However, to counter this negative kinetic energy propellant mass fraction, the increase in altitude and the entropy generation due to drag would then cause the sum of the propellant mass fractions associated with altitude and losses to proportionally increase. Negative propellant mass fractions as analytically defined here (in terms of either kinetic energy or potential energy changes) are therefore simply indicative of the necessary and inevitable thermodynamic flow of availability between these three modes (kinetic energy change, altitude change and losses).

The altitude integral in Eq. (18) and in subsequent development can be approximately modeled (assuming constant $\dot{m}_p$ and negligible change in g) as follows:

$$\int_{h_{\text{initial}}}^{h_f} m_{\text{veh}} g \, \mathrm{d}h = \left[m_{\text{veh(initial)}} - \frac{\Delta(\text{propellant mass used})}{2} \right] g(h_f - h_{\text{initial}}) \tag{30}$$

Here h_{initial} and h_f are the initial and final altitudes, respectively. This approximation is well-suited for many rocket applications (i.e. across

the burn of a given stage); less suitable for air-breathing configurations. For illustration purposes, however, the modeling described in Eq. (30) is used for the analysis of propellant mass fractions later in this section, for both rocket and air-breathing configurations.

Using this approximation and defining a mission in which both initial vehicle velocity and initial altitude (V_{initial} and h_{initial}) are equal to zero and V_f and h_f are the final velocity and altitude, respectively, the following expressions for the vehicle propellant mass fractions for kinetic energy and potential energy changes and propellant mass fraction required to overcome irreversibilities are written:

$$\lambda_{P,\text{KE}} = \frac{V_f^2}{2H_P}(1-\lambda_P) \tag{31}$$

$$\lambda_{P,\text{PE}} = \frac{gh_f}{H_P}\left(1-\frac{\lambda_P}{2}\right) \tag{32}$$

$$\lambda_{P,\text{LOSS}} = \frac{\int_{\text{mission}} T_i \, \text{d}S_{\text{irr(total)}}}{H_P m_{\text{veh(initial)}}} = \lambda_P - \lambda_{P,\text{KE}} - \lambda_{P,\text{PE}} \tag{33}$$

This indicates that the vehicle propellant mass fraction can be subdivided into three contributions as demonstrated in Eqs. (25) and (33): 1) propellant fraction necessary to effect the kinetic energy change across the mission, 2) propellant fraction necessary to effect altitude change from initial to final altitude (i.e. potential energy change across the mission), and 3) propellant fraction associated with (or available for) overcoming all irreversibilities both in and over the aerospace vehicle and in the vehicle wake.

A. Single-Stage-to-Orbit Comparison Based on Second-Law Analysis

The overall mass of an aerospace vehicle can be considered to be the sum of the propellant mass, the structural/system mass (sometimes termed the dead weight mass), and the payload mass, i.e.,

$$1 = \lambda_p + \lambda_d + \lambda_l = \lambda_p + \frac{\text{structure/system mass}}{m_{\text{veh(initial)}}} + \frac{\text{payload mass}}{m_{\text{veh(initial)}}} \tag{34}$$

As a simple example using the foregoing analysis [specifically based on Eq. (31–33)], consider the propellant mass fraction characteristics for two SSTO vehicles, the first propelled by a H_2-O_2 rocket and the second by an air-breathing H_2-fueled propulsion system or systems. Let the required altitude change be 300,000 m at a required final velocity of 7900 m/s. The approximate heating value of stoichimetric H_2-O_2 combustion is taken as 1.34×10^7 J/kg (propellant) and the approximate heating value of H_2 in air is taken as 1.2×10^8 J/kg (fuel).

Figure 4 provides a plot of the mass fraction breakdown versus overall propellant mass fraction for the SSTO mission for a H_2-O_2 rocket with characteristics as defined above. Specifically, the overall propellant mass fraction is the sum of the propellant mass fractions necessary for kinetic energy change, potential energy change, and overcoming losses. Note that (for instance) for an overall propellant mass fraction of 0.8, the sum of the dead weight and payload mass fractions as defined above would be 0.2, by definition. The most interesting result displayed on this figure are the characteristics of the propellant mass fraction specifically available to the vehicle for overcoming irreversibilities. Note that this quantity rapidly approaches zero for decreasing overall propellant mass fraction such that there is no propellant mass fraction available for overcoming any losses for an overall propellant mass fraction less than approximately 0.75. In other words, any H_2-O_2 SSTO rocket configuration proposed or imagined with smaller overall propellant mass fraction than 0.75 is thermodynamically impossible (representing a violation of the laws of nature). Furthermore, a real rocket system will actually require that a considerable fraction of its propellant be used to overcome losses, both internal and external (i.e. the second-law limit illustrated on this figure is the absolute limit, not the practical/feasible

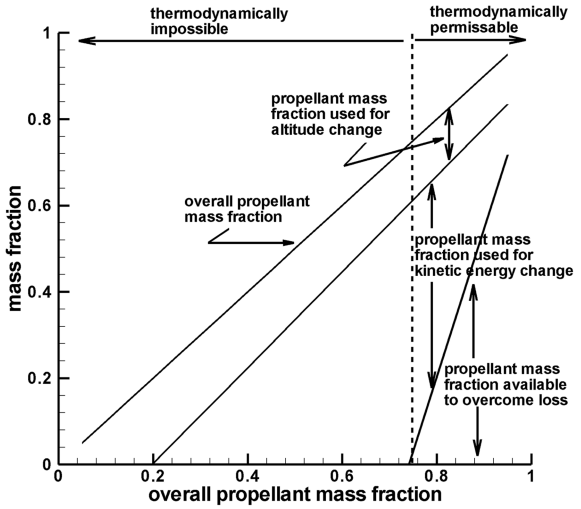

Fig. 4 Propellant mass fraction breakdown for SSTO H_2-O_2 rocket mission.

limit); it is thus not encouraging to observe the rapidly constricting envelope of available payload/dead weight mass for larger and more meaningful values of propellant required to overcome irreversibility. For example, if a meaningful mass ratio of structure plus payload is taken as 0.2, this means that less than 6% of the initial propellant mass at launch is available to overcome irreversibility from launch to orbit.

Figure 5 shows a similar breakdown for a SSTO H_2–air (air-breathing) mission. There is significantly greater propellant mass fraction available to the vehicle for overcoming losses, as compared with the SSTO rocket. Therefore the range of thermodynamically possible configurations is much expanded over the rocket configuration (i.e. for the air-breathing SSTO vehicle there is no thermodynamically possible configuration for any overall propellant mass fraction less than approximately 0.25). However, due to the expected higher irreversibility for air-breathing SSTO (due to long duration accelerating trans-atmospheric flight), such a configuration would, of course, need at least some of this margin and probably a good deal more than is available. Note also that the simplified modeling of the potential energy term used in the generation of these results [Eq. (33)] is not very accurate for such an air-breathing configuration and mission. (Again, however, the propellant mass fraction associated with the altitude change is generally smaller than

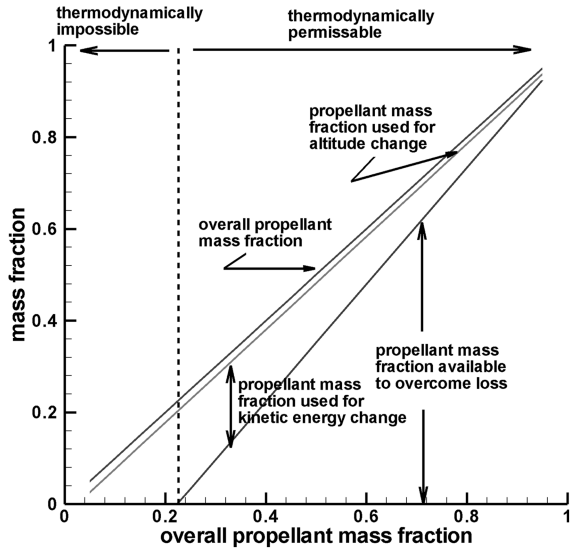

Fig. 5 Propellant mass fraction breakdown for SSTO H_2–air air-breathing mission.

the propellant mass fractions associated with kinetic energy change and losses.)

B. Apollo Access-to-Space Example (Second-Law Analysis)

The following simplified example provides the total irreversibility generated for the three stages of a nominal Apollo mission profile from launch to achievement of the parking orbit (preliminary to stage 3 refiring for initiating the trip to the moon). The following configuration and parameters were used (note the effective heating values are roughly approximated based on the given specific impulses and thrusts):

In stage 1 (RP1-LOX), overall mass = 2, 920, 000 kg, propellant mass = 2, 150, 000 kg, empty mass of stage and connector = 136, 000 kg, overall thrust = 34, 000, 000 N, burn time = 170 s, altitude achieved = 61 km, mass flow rate of propellant = 12, 600 kg/s, specific impulse = 303 s/(274 s effective), heating value of propellant (estimated) = 8.0×10^6 J/kg, and V(final) = 2682 m/s. In stage 2 (LH2-LOX), overall mass = 640, 000 kg, propellant mass = 444, 000 kg, empty mass of stage and connector = 40, 000 kg, overall thrust= 4, 450, 000 N, burn time = 395 s, altitude achieved = 184 km, mass flow rate of propellant = 1125 kg/s, specific impulse= 453 s/(403 s effective), heating value of propellant (estimated)= 1.19×10^7 J/kg, and V(final) = 6838 m/s. In stage 3 (LH2-LOX), overall mass = 156, 000 kg, propellant mass = 37, 000 kg, overall thrust = 890, 000 N, burn time = 165 s, altitude achieved= 185 km, mass flow rate of propellant = 222 kg/s, specific impulse = 453 s/(403 s effective), heating value of propellant (approximated) = 1.19×10^7 J/kg, and V(final) = 6838 m/s.

Equations (18) and (30) are then used to estimate the total irreversibility generated by the Apollo stack across the defined mission with the following results:

Stage 1: availability loss due to irreversibilities = 1.33×10^{13} Joules

Stage 2: availability loss due to irreversibilities = 2.5×10^{12} Joules

Stage 3: availability loss due to irreversibilities = 1.3×10^{12} Joules

Total availability loss due to irreversibilities = 1.7×10^{13} Joules

Total work due to kinetic energy change = 4.2×10^{12} Joules

Total work due to altitude change = 1.6×10^{12} Joules

Total propellant energy expended = 2.3×10^{13} Joules

This analysis indicates that approximately 74% of the total propellant energy expended by the Apollo stack system from launch to parking orbit was necessary to overcome availability losses (irreversibility) in the mission. Nineteen and 7% of the total propellant energy went to realizing the desired kinetic energy and the desired altitude changes of the mission, respectively.

V. Availability Loss Rate Description for Aerospace Vehicles

This section analyzes overall availability losses in terms of instantaneous rate contributions due to vehicle acceleration, climb (potential energy changes) and atmospheric cruise. Equation (4) provides the availability-performance relationship and is repeated here for convenience:

$$F_{x(\text{flight})}V = \dot{m}_p\left[\frac{V^2}{2} + H_P\right] - T_i\dot{S}_{\text{irr(total)}}$$

This relationship provides an instantaneous balance equation describing the balance between accelerative force on the vehicle, energy content associated with propellant expended, and the availability loss rate due to irreversibilities. It is of interest to examine this relationship in more detail from the standpoint of the drivers on the availability loss rate at any given instant. Of specific interest is the instantaneous availability loss per kilogram of vehicle mass, denoted as β. This parameter is defined as

$$\beta = \frac{T_i\dot{S}_{\text{irr(total)}}}{m_{\text{veh}}} \tag{35}$$

The mass flow rate of propellant is defined in terms of the engine thrust and the specific impulse of the propulsion system as follows:

$$\dot{m}_p = \frac{\text{Thrust}}{I_{\text{sp}}g_0} \tag{36}$$

Engine thrust as given in Eq. (36) and as used for engine specific impulse rating is usually defined as Thrust $= \dot{m}_P(u_e - u_i) + (P_e - P_i)A_e$. Formally this represents the net force component along the main engine axis experienced by the internal wetted surfaces of the engine along with a contribution from an external cowling exposed to uniform external pressure P_i. Assuming small α_T in Fig. 3, the axial (flight-path direction) force experienced by all internal wetted surfaces of the engine is $F_{x(\text{engine})}$ where $F_{x(\text{engine})} = \dot{m}_P(u_e - u_i) + (P_eA_e - P_iA_e)$. Therefore, although $F_{x(\text{engine})}$ is formally equal to Thrust $+ (A_e - A_i)P_i$, the simplifying assumption will be made in the following analysis that $F_{x(\text{engine})}$ = Thrust from the standpoint of using the rated specific impulse for rocket and air-breathing engines.

The general situation of interest for an aerospace vehicle is the case in which the vehicle is flying in the atmosphere with some instantaneous values of 1) external aerodynamic drag D, 2) given acceleration a_{veh}, and 3) given climb angle θ. Initially, however, three special availability loss rate cases are examined in terms of the (D, a_{veh}, θ) characteristics of the vehicle. The availability loss rate characteristics of an accelerating, climbing vehicle in flight in the atmosphere are then derived.

A. Atmospheric Nonaccelerating, Nonclimbing Vehicle ($D, a_{\text{veh}} = 0, \theta = 0$)

First consider the specific case where the vehicle is in a flight condition with the given drag, D; however with zero acceleration, i.e. $a_{\text{veh}} = 0$, and no component of vehicle weight in the direction of flight such that $\theta = 0$ (zero climb angle). The following is written:

$$F_{x(\text{flight})} = F_{x(\text{engine})} - D = m_{\text{veh}}a_{\text{veh}} = 0 \tag{37}$$

Therefore,

$$0 = \left[\frac{V^2}{2} + H_P\right]\frac{F_{x(\text{engine})}}{I_{\text{sp}}g_0} - T_i\dot{S}_{\text{irr(total)}} \tag{38}$$

Hence, assuming $g = g_0$,

$$\beta(\text{drag, no acceleration, no climb}) = \frac{H_P + V^2/2}{I_{\text{sp}}}\left[\frac{D}{m_{\text{veh}}g_0}\right] = \frac{H_P + V^2/2}{I_{\text{sp}}}\left[\frac{D}{W}\right] \tag{39}$$

B. Acceleration in Absence of Drag and Without Climbing ($D = 0, a_{\text{veh}}, \theta = 0$)

For constant altitude acceleration in the absence of external drag,

$$F_{x(\text{flight})} = F_{x(\text{engine})} = m_{\text{veh}}a_{\text{veh}} \tag{40}$$

Insertion of this model into Eq. (4) with manipulation yields the following expression:

$$\beta(\text{accelerating, no drag, no climb}) = a_{\text{veh}}\left[\frac{H_P + \frac{V^2}{2}}{I_{\text{sp}}g_0} - V\right] \tag{41}$$

C. Climbing Flight Without Acceleration and Without Drag ($D = 0, a_{\text{veh}} = 0, \theta$)

For climbing flight without acceleration and without external drag the equation of motion in the flight-path direction is: $F_{x(\text{engine})} = F_{x(\text{flight})} = m_{\text{veh}}g\sin\theta$

This then yields [when combined with Eqs. (4) and (35)] the following:

$$\beta(\text{climb, no drag, no acceleration}) = g\sin\theta\left[\frac{H_P + \frac{V^2}{2}}{I_{\text{sp}}g_0} - V\right] \tag{42}$$

D. General Case: Accelerating Vehicle in Climbing Flight in the Atmosphere

Referring to Fig. 3, it can be seen that the following are the general equations of motion for an accelerating, climbing vehicle in the atmosphere (without centripetal acceleration):

$$F_{x(\text{engine})} = D + W\sin\theta + m_{\text{veh}}a_{\text{veh}} \qquad W\cos\theta = L \tag{43}$$

By definition,

$$F_{x(\text{flight})} = F_{x(\text{engine})} - D \tag{44}$$

Hence,

$$Vm_{\text{veh}}g\sin\theta + Vm_{\text{veh}}a_{\text{veh}} = \left(H_P + \frac{V^2}{2}\right)\frac{F_{x(\text{engine})}}{I_{\text{sp}}g_0} - T_i\dot{S}_{\text{irr(total)}} \tag{45}$$

This expression can then be rearranged to yield the following result:

$$\beta(\text{general vehicle; accelerating, climbing, with external drag}) = A + B + C \tag{46}$$

where

$$A = \frac{(H_P + \frac{V^2}{2})}{I_{\text{sp}}}\frac{D}{m_{\text{veh}}g_0} = \frac{(H_P + \frac{V^2}{2})}{I_{\text{sp}}}\left[\frac{D}{W}\right]$$

$$B = g\sin\theta\left[\frac{H_P + \frac{V^2}{2}}{I_{\text{sp}}g_0} - V\right] \qquad C = a_{\text{veh}}\left[\frac{H_P + \frac{V^2}{2}}{I_{\text{sp}}g_0} - V\right] \tag{47}$$

or

$$\beta = \beta(\text{cruise in atmosphere}) + \beta(\text{accelerating, no drag, no climb}) + \beta(\text{climb, no drag, no acceleration}) \tag{48}$$

This indicates that there exists a convenient superposition principle when describing the general case of the overall availability loss rate for an accelerating, climbing vehicle in the atmosphere with given characteristics (D, a_{veh}, θ). Specifically this availability loss rate is the sum of the separate availability loss rates for 1) the vehicle in atmospheric cruise with a given drag, 2) the vehicle in steady climb with climb angle θ against a gravitational field but without atmospheric drag, and 3) the vehicle accelerating at a_{veh} in the absence of drag and gravity effects. Hence contribution A (above) is the availability loss due to irreversibilities solely associated with overcoming the given external aerodynamic drag D at a specified velocity (including drag due to generation of required lift, if any); without acceleration and without consideration of gravity (i.e. as if the vehicle is in constant altitude cruise). Contribution B is the availability loss due to irreversibilities in the absence of acceleration and external drag when there is a component of vehicle weight aligned with the aerodynamic force vector, i.e., when the vehicle is in a steady climb in a gravitational field without drag at the given climb angle θ. Contribution C is the availability loss due to irreversibilities associated solely with the given acceleration a_{veh} of the vehicle, as if it occurred in the absence of atmospheric drag and gravitational effects. Note that these increments are inclusive of the wake generation of entropy associated with each increment.

For the general case of an accelerating and climbing vehicle contributions A and B can also be written in terms of the L/D ratio and the rate of climb ($R/C = V\sin\theta$) such that

$$A = \frac{(H_P + \frac{V^2}{2})}{I_{\text{sp}}}\frac{D}{m_{\text{veh}}g_0} = \frac{(H_P + \frac{V^2}{2})}{I_{\text{sp}}}\left[\frac{D}{W}\right] = \frac{(H_P + \frac{V^2}{2})}{I_{\text{sp}}}\frac{\cos\theta}{(\frac{L}{D})}$$

$$B = g\sin\theta\left[\frac{H_P + \frac{V^2}{2}}{I_{\text{sp}}g_0} - V\right] = (R/C)g\left[\frac{\frac{H_P}{V} + \frac{V}{2}}{I_{\text{sp}}g_0} - 1\right]$$

$$C = a_{\text{veh}}\left[\frac{H_P + \frac{V^2}{2}}{I_{\text{sp}}g_0} - V\right]$$

Therefore increasing L/D is beneficial in terms of decreasing losses whereas increasing R/C or increasing climb angle generally increases losses through the increase in contribution B above.

E. Example: Constant Altitude Acceleration, Availability Loss Rate per kg of Vehicle Mass

The preceding analysis is developed in terms of engine specific impulse, or I_{sp}. Figure 6 shows the well-known nominal specific impulses versus flight Mach number for various classes of aerospace engines corresponding to air-breathers, both hydrogen-fueled and hydrocarbon-fueled, and rockets (H_2-O_2). These values can be approximated by simple curve-fits through the average I_{sp} and then used within the previous analysis in order to provide a broad assessment of the performance characteristics and comparisons for classes of vehicles across the flight Mach number range.

As an example illustrating the previous analysis, the relevant terms in Eq. (47) are plotted for an accelerating H_2-O_2 rocket-powered vehicle at constant altitude of 30 km (climb angle = 0). The overall β is plotted as the sum of both discrete increments associated with 1) the cruise contribution A or β (cruise in atmosphere) and 2) the acceleration contribution B or β (acceleration, no drag, no climb) versus flight Mach number in Fig. 7. The specific impulse is assumed to be 460 s and the D/W ratio (for the cruise loss component) is 0.333.

The relationship is plotted for three different values of vehicle acceleration; the first is the (lowest) baseline zero acceleration case corresponding to the cruise only (drag) loss curve. This baseline curve is invariant for losses incurred for any vehicle acceleration, i.e., the total availability loss rate is the sum of the cruise (zero acceleration) data and the acceleration loss for a given acceleration (here shown for 2 and 10 m/s^2). A significant feature of this plot is the minimum observed in the overall availability loss rate (loss in availability) which occurs for higher accelerations at a Mach number of approximately 11.5 (for the given configuration). This fact demonstrates the tradeoff that exists between decreasing acceleration losses and increasing cruise/drag losses as flight Mach is increased; this trade results in the minimum-loss Mach number for higher accelerations. The characteristics of the minimum-loss flight Mach number for rocket-powered vehicles are discussed more in the next section of this document.

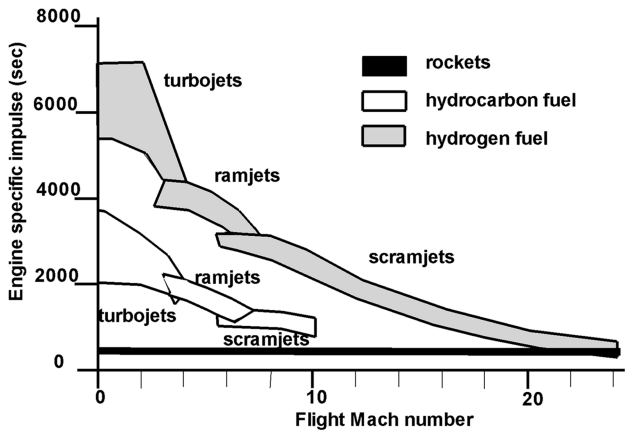

Fig. 6 Nominal specific impulses versus flight Mach number for various propulsion systems.

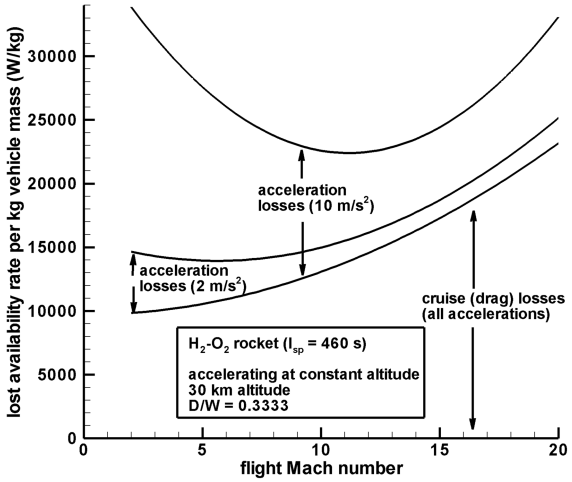

Fig. 7 H_2-O_2 rocket-powered vehicle accelerating at constant altitude; lost availability rate (β) versus flight Mach number in terms of acceleration and drag contributions.

Figure 8 plots the overall availability loss rate per kilogram of vehicle mass for a hydrogen-fueled air-breathing vehicle versus flight Mach number using Eq. (47). Like the rocket-powered vehicle analyzed in Fig. 7, this vehicle is in constant altitude and accelerating flight at a D/W ratio $= 0.333$ and an altitude of 30 km (i.e. the vehicle is not climbing, such that $\theta = 0$). As noted earlier, the Mach number dependence of the specific impulse for such a vehicle is approximated using simple curve-fits from the data shown in Fig. 6. Results are shown for two vehicle accelerations as shown (zero and 2 m/s^2). The overall availability loss rate per kilogram of vehicle mass is again seen to be the sum of the acceleration loss and the cruise (drag) loss; again the latter loss is invariant with the amount of vehicle acceleration. Unlike the rocket-powered vehicle, however, there is no minimum-loss Mach number, i.e., the overall loss increases with increasing flight Mach number across the range.

VI. Minimization of Overall Lost Availability Rate for Aerospace Vehicles

This section describes the methodology necessary for separating the overall availability loss rate for a vehicle into two main contributions: the vehicle external drag power and the power loss associated with the propulsion system (with both contributions inclusive of related wake effects and representing loss in global availability.) It should be noted that the previous section provided analysis which showed that overall availability loss rate per unit vehicle mass for an accelerating climbing vehicle in the atmosphere could be found by the superposition of three distinct contributions corresponding to cruise (no acceleration, no climb), acceleration (no drag, no climb) and climb (no drag, no acceleration). The approach in this section provides a complementary examination in which the losses of availability are described in terms of the fundamental balance between losses attributable to external aerodynamic losses and internal propulsion system losses.

Equation (4) is written as follows:

$$(F_{x(\text{engine})} - D)V = \frac{F_{x(\text{engine})}}{g_0 I_{\text{sp}}}\left(\frac{V^2}{2} + H_P\right) - T_i \dot{S}_{\text{irr(total)}} \tag{50}$$

This is rearranged to yield

$$T_i \dot{S}_{\text{irr(total)}} = (DV) + (F_{x(\text{engine})}V)\left\{\left(\frac{1}{g_0 I_{\text{SP}}}\right)\left[\frac{V}{2} + \frac{H_P}{V}\right] - 1\right\} \tag{51}$$

This relationship demonstrates that the instantaneous overall availability loss rate for an aerospace vehicle is the summation of the drag power expended by the vehicle plus the loss contribution associated with the propulsion system (proportional to the thrust power).

A. Availability Loss Rate for Rocket-Powered Vehicles

The external drag for a rocket-powered vehicle can be modeled using a drag coefficient C_D based on frontal cross-sectional area of the vehicle, A_{frontal} such that

$$D = C_D\left(\frac{1}{2}\rho_i V^2\right)A_{\text{frontal}} \tag{52}$$

The total availability loss rate per meter of frontal cross-sectional area of a vehicle is then written as

$$\frac{T_i \dot{S}_{\text{irr(total)}}}{A_{\text{frontal}}} = \left(C_D \frac{1}{2}\rho_i V^3\right) + \left(\left[\frac{F_{x(\text{engine})}}{A_{\text{frontal}}}\right]V\right)\left\{\left(\frac{1}{g_0 I_{\text{SP}}}\right)\left[\frac{V}{2} + \frac{H_P}{V}\right] - 1\right\} \tag{53}$$

This relationship is plotted (using unit cross-sectional area) versus flight Mach number in Fig. 9 for a H_2-O_2 rocket-powered vehicle with specific impulse of 460 s at 30 km altitude, assumed heating value of 1.34×10^7 J/kg (propellant) and drag coefficient of 0.3 (fixed). The parameter $F_{x(\text{engine})}/A_{\text{frontal}} =$ thrust$/A_{\text{frontal}}$ in Eq. (53) was estimated (in order to provide generic rocket characteristics for demonstration) at 300, 000 N/m^2 based on examining a range of large high thrust-to-weight rockets such as the Pegasus (350,000), Titan (320,000), Trident (362,000), Atlas (219,000), and Saturn V

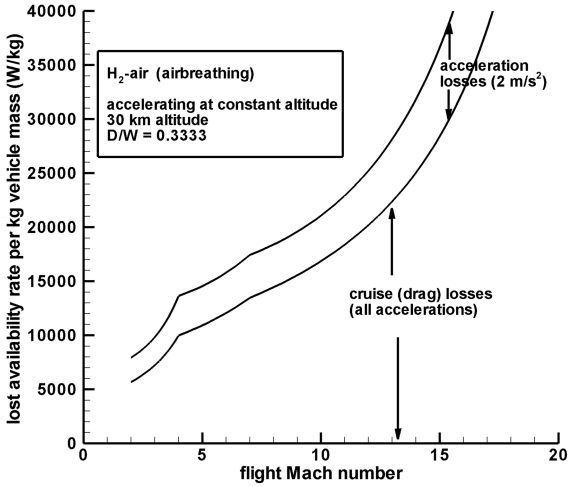

Fig. 8 H_2–air air-breathing vehicle accelerating at constant altitude; lost availability rate (β) in terms of acceleration and drag contributions versus flight Mach number.

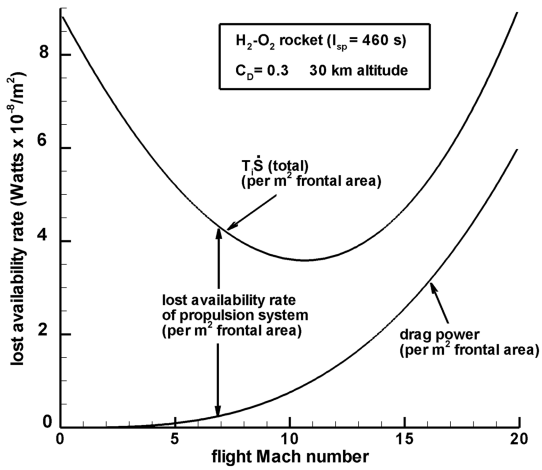

Fig. 9 Overall availability loss rate (Watts x 10^{-8} per m^2 of vehicle frontal area) versus flight Mach number for rocket-powered vehicle at indicated conditions (thrust$/A_{\text{frontal}} = 300000$ N/m^2).

(424,000). Note that Eq. (53) is valid for an accelerating and climbing vehicle at a given altitude (i.e. no assumption of cruise is mandated in its development). Figure 9 illustrates the two contributions in Eq. (53); the total availability loss rate per meter of frontal area is the sum of the drag power term and the propulsion loss term. Figure 10 plots for the same case the contributions versus flight Mach number using the specific balance in Eq. (51), i.e., in terms of (thrust-drag) power, overall expended power and loss work rate.

Figure 9 and 10 illustrate that, for a rocket-powered vehicle at a given altitude, there is a specific flight velocity at which the overall availability loss rate is minimized. This minimum-loss point was observed earlier in the examination of the availability loss per kilogram of vehicle mass (see Fig. 7). The flight Mach number for minimal overall availability loss for a rocket-powered vehicle can be found by differentiating the availability loss rate with respect to velocity at given engine thrust levels. This results in the following quadratic equation for optimal (minimum-loss) velocity:

$$\left\{\frac{3}{2}C_D\rho_i\right\}V^2_{(\text{min-loss})} + \left\{\left(\frac{F_{x(\text{engine})}}{A_{\text{frontal}}}\right)\frac{1.}{g_0 I_{\text{sp}}}\right\}V_{(\text{min-loss})} - \left(\frac{F_{x(\text{engine})}}{A_{\text{frontal}}}\right) = 0 \tag{54}$$

The resulting distributions of the optimal (minimum-loss) flight velocities (corresponding to optimal flight Mach numbers) versus altitude for four different drag coefficients are plotted in Fig. 11. The density is modeled using a simple exponential approximation through the atmosphere. Figure 11 also illustrates that the maximum velocity beyond which the overall availability loss rate for a rocket is inevitably greater than the minimum possible overall availability loss rate is around 4500 m/s, corresponding to about Mach 14. Note that this analysis is based on total availability loss rate per unit (frontal) cross-sectional area of the vehicle.

Figure 12 plots contours of instantaneous availability loss rates per m^2 frontal area associated with this same rocket-powered vehicle configuration ($C_D = 0.3$, H_2-O_2, assumed heating value of 1.34×10^7 J/kg (propellant) and thrust/$A_{\text{frontal}} = 300,000$ N/m^2) for flight velocities ranging from 0 to 7000 m/s and altitudes ranging from 0 to 180 km. This figure provides a unique assessment of the loss characteristics across the entire flight envelope and demonstrates the intriguing existence of a minimum-loss rate column centered at around 4500 m/s flight velocity and extending from 50 km altitude to orbital altitudes. In this column overall loss rates are very low; entropy generation rates for flight in this zone are much smaller than anywhere else in the velocity-altitude range. In addition, there is a minimum-loss rate corridor extending from the lower left-hand corner region of low velocity, low altitude flight to the lower reaches of this low-loss rate column. If a rocket-powered design was in general to take advantage of this higher velocity-lower altitude corridor, it presumably would be required to provide some significant lift from lifting surfaces or thrust vectoring (over that of most current systems). As discussed earlier, the details of loss characteristics in the flight velocity-altitude space are driven by the various trades existing in Eq. (53); i.e. between high drag losses at high flight velocity and high propulsion system losses at low flight velocity.

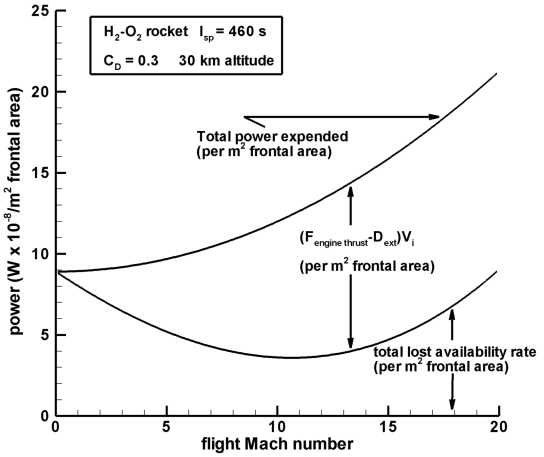

Fig. 10 Total power expended (Watts x 10^{-8} per m^2 of vehicle frontal area) versus flight Mach number for rocket-powered vehicle at indicated conditions (thrust/$A_{\text{frontal}} = 300000$ N/m^2); balance contributions from Eq. (50).

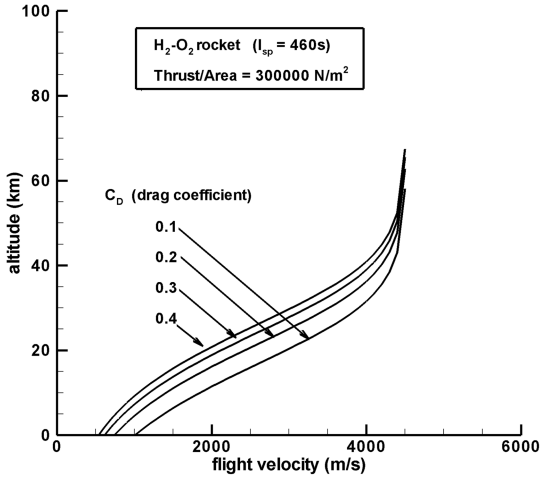

Fig. 11 Optimal (minimum overall loss rate) velocity versus altitude for H_2-O_2 rockets (availability-based).

It is important to clarify what the contours in Fig. 12 show (and what they do not show). Recall from Eq. (18) that minimum overall losses generated across a mission correspond to maximum vehicle performance in terms of achieved kinetic energy and altitude. This means that a vehicle that spends a relatively short time in a high-loss rate altitude-velocity region (as depicted on Fig. 12) may have less overall (time-integrated) loss and hence better performance than a vehicle that spends a relatively long time in a low-loss rate region. Figure 12, which provides contours of loss rate, does not address this critical issue of time-integration of losses. In addition, this plot is generated for specific rocket characteristics (i.e. $C_D = 0.3$, thrust/$A_{\text{frontal}} = 300,000$ N/m^2, H_2-O_2, and assumed heating value of 1.34×10^7 J/kg (propellant)). The details of the contours themselves change depending on how, for instance, the drag coefficient changes during the flight of a given vehicle. The location and span of the low-loss region in higher velocity-altitude space is particularly sensitive to the heating value of the propellant and to the engine specific impulse. Nevertheless, the type of information provided in Fig. 12 provides a powerful tool for understanding and evaluating optimization for rocket-powered flight in terms of the single parameter of entropy generation. This is especially true when it is coupled with a time-integration approach in order to determine or estimate actual time-integrated losses.

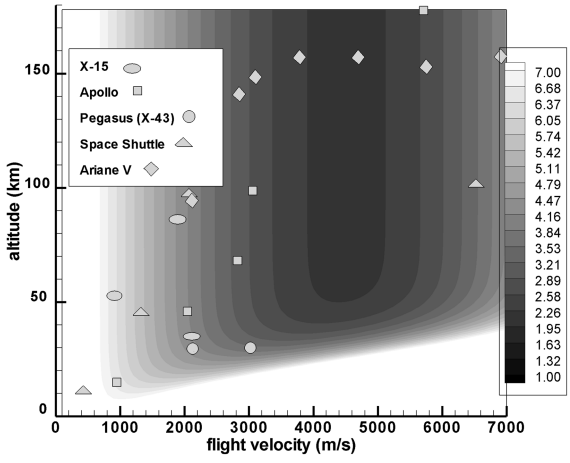

Fig. 12 Contours of availability loss rate (availability loss in W x 10^{-8}) per m^2 of frontal area plotted in terms of flight velocity and altitude; for H_2-O_2 rocket, $I_{\text{sp}} = 460$ s, $C_D = 0.3$, thrust/$A_{\text{frontal}} = 300,000$ N/m^2.

Also shown in Fig. 12 are some representative flight velocity-altitude points for a range of large rocket systems (mostly comprising access-to-space systems). However these systems do not correspond to the generic configuration for which the underlying contours are plotted, i.e. C_D, thrust/A_{frontal}, type of propellant, I_{sp} differ. They are shown only for reference purposes.

B. Availability Loss Rate for Air-Breathing Engine-Powered Vehicles

Although the analysis developed in the previous section is valid for both rocket-powered and air-breathing engine-powered vehicles, it is useful to examine the air-breathing case differently since engine axial force (thrust) is dependent on air mass captured by the inlet and hence has explicit flight Mach number dependence. Equation (4) can be written for a vehicle with an air-breathing engine system as follows:

$$(F_{x(\text{engine})} - D)V + T_i\dot{S}_{\text{irr(total)}} = \rho_i V A_{\text{cap}} f\left[\frac{V^2}{2} + H_P\right] \tag{55}$$

A_{cap} is the frontal air capture area associated with the propulsion system and can be defined as a percent of vehicle (frontal) cross-sectional area, A_{frontal}. f is the fuel–air ratio; for H_2–air combustion, the stoichimetric fuel–air ratio, f_{stoich}, is equal to 0.029. As a very simple model at higher flight Mach numbers that accounts approximately for the flight Mach number dependence on injected f (in order to account for the fuel flow rate required for cooling), the following expression is used for flight Mach greater than 10:

$$f = f_{\text{stoich}} \cdot (M_i/10) \tag{56}$$

For calculation of actual engine thrust using the specific impulse, however, the fuel–air ratio is capped at the stoichimetric value (here neglecting mass/injection effects on engine thrust). The right-hand side of Eq. (55) is the power price paid by the vehicle from the standpoint of a stationary observer. It is the summation of the net force-power experienced by the vehicle and the availability loss rate.

The expression in Eq. (55) can also be manipulated (where C_D is again referenced to the frontal cross-sectional area of the vehicle) to yield

$$\frac{T_i\dot{S}_{\text{irr(total)}}}{A_{\text{frontal}}} = \left(C_D\frac{1}{2}\rho_i V^3\right) + \rho_i V\frac{A_{\text{cap}}}{A_{\text{frontal}}}\left[f\left\{\frac{V^2}{2} + H_P\right\} - f_{\text{stoich}} I_{\text{sp}} g_0 V\right] \tag{57}$$

An example H_2–air air-breathing vehicle is analyzed using Eq. (57) at conditions corresponding to an altitude of 30 km; results are plotted in Fig. 13. For this example, a constant vehicle drag coefficient of 0.3 and a constant capture area to frontal area ratio of 0.8 were used. Air-breathing engine specific impulse variation with flight Mach number was approximated from Fig. 6; altitude effects on specific impulse are not considered here. Unlike the rocket (analyzed with constant thrust and propellant flow rate), there is no minimum-loss flight Mach number for the air-breathing configuration which has thrust levels continuously increasing with flight Mach numbers. The overall availability loss rate per unit frontal area (as well as both of its constituent contributions from drag power and propulsion system loss) exponentially increases with flight Mach number.

Figure 14 is a plot of power increments as given in Eq. (55), i.e., overall loss rate, expended power and thrust-drag power versus flight Mach number for the same vehicle. It is seen that the maximum accelerative (i.e. cruise) flight Mach number for this configuration occurs at about 11 due to the drag power exceeding the thrust power for higher Mach numbers. Equivalently, as seen on this Figure, this occurs when overall loss rate due to irreversibility exceeds expended power provided by the vehicle. There are very small thrust-to-drag power margins, and hence limited acceleration, available to the air-breathing vehicle as compared with rocket-powered vehicles, as demonstrated here.

Figure 15 plots contours of instantaneous availability loss rates per m^2 frontal area associated with this same air-breathing vehicle configuration ($C_D = 0.3$, H_2–air) for flight velocities ranging from 0 to 7000 m/s and altitudes ranging from 0 to 180 km. The loss rate characteristics for the air-breathing configuration are straightforwardly dominated by the high drag occurring at higher flight velocities and low altitudes; there are no embedded low-loss rate regions observed within the contours as was seen in the rocket example previously examined. However, it is obvious from this Figure that an air-breathing configuration must in some sense ride over the high-loss rate region. At the same time, however, it must maintain a low enough altitude for the generation of adequate lift (thrust-to-weight ratios being small for the air-breathing vehicle) and in order to maintain adequate engine operability margins.

Again, it is important to emphasize that, although loss rates as shown are in general considerably smaller for air-breathing vehicles than for rocket-powered vehicles (compare Fig. 12–15), optimization across a mission is due to the minimization of the overall time-integrated entropy generation/loss characteristics. The time of flight for rockets with their intrinsically high thrust/area and high accelerations is much smaller in general than for air-breathing vehicles. Hence a rocket which inevitably operates in a higher-loss rate scenario for relatively short duration can conceivably generate less overall losses than an air-breathing vehicle which operates in a lower-loss rate scenario for longer duration. For reference purposes, a representative SSTO air-breathing trajectory is sketched on this plot along with the constant dynamic pressure line corresponding to 2000 psf. Note that constraints on the possible flight envelope due to high heating (higher dynamic pressures) correspond to the

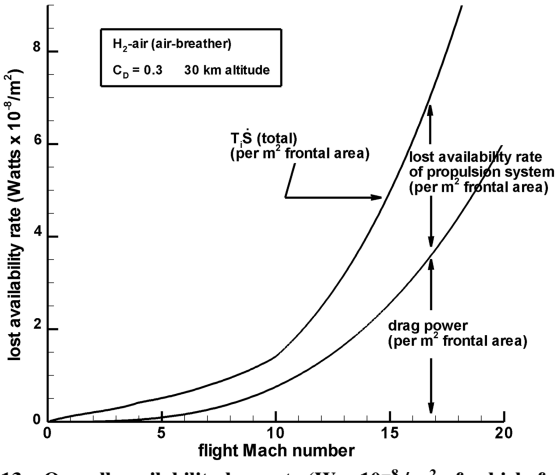

Fig. 13 Overall availability loss rate (W x $10^{-8}/m^2$ of vehicle frontal area) for air-breathing vehicle with indicated conditions.

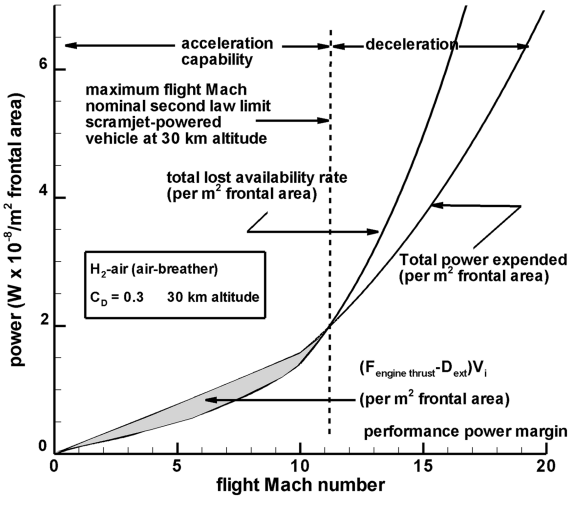

Fig. 14 Power considerations (showing maximum theoretical flight Mach number) for air-breathing vehicle.

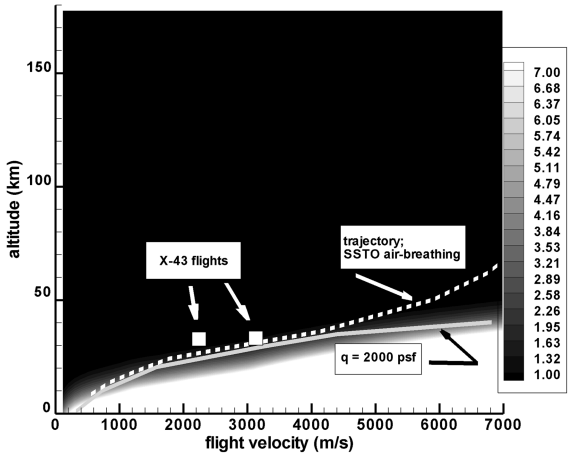

Fig. 15 Contours of availability loss rate (availability loss in W × 10^{-8} per m^2 frontal area) plotted in terms of flight velocity and altitude; for air-breathing vehicle with H_2–air propulsion system, $C_D = 0.3$.

constraints due to high loss rates. Finally, the two approximate performance points for the Mach 7 and Mach 10 flights of the X-43 are overlaid on the contours in Fig. 15.

VII. Conclusions

This paper demonstrates that the general availability rate balance for an aerospace vehicle can be analytically combined with the vehicle equations of motion in order to obtain instantaneous rate descriptions for losses and energy use. These rate relationships can be then integrated across the time of mission such that the fundamental analytic balance is obtained between 1) the overall vehicle energy usage in terms of energy associated with propellant expended during the mission, 2) the resultant vehicle kinetic energy and potential energy changes, and 3) the resultant lost availability due to the generation of entropy throughout the time of the mission, including within the wake. This analysis is then put in terms of the effective contributions of these attributes (kinetic energy changes, altitude changes and required availability losses) to the overall vehicle propellant mass fraction. Simple examples are shown using this methodology; these examples describe results of the analysis for hypothetical SSTO rocket-powered and air-breathing configurations. SSTO rocket systems are shown to be at best problematic from the most fundamental considerations of entropy generation; specifically no chemical rocket-based system with less than 75% overall propellant mass fraction is even thermodynamically possible. In addition, for an optimistic scenario of 80% propellant mass fraction (leaving only 20% overall initial system mass available for vehicle and payload), only around 6% of the overall propellant mass would be available for overcoming all losses associated with all system irreversibility which occurs throughout the entire access-to-space mission. For the air-breathing SSTO system, there is far greater margin in the possible propellant mass fraction envelope. Specifically, the minimum propellant mass fraction below which the air-breathing SSTO system is thermodynamically impossible is 20%. In addition, for a propellant mass fraction of 60% (corresponding to 40% initial system mass available for vehicle structure and payload), propellant mass fraction available for overcoming all losses due to irreversibility throughout the access-to-space mission is approximately 35%. However, the air-breathing SSTO system is also inherently problematic due to the fact that it has (at best) relatively low acceleration characteristics and hence will need considerably longer times in the atmosphere. Hence, losses will steadily accumulate over these longer mission times such that large propellant mass fractions associated with overcoming losses will be necessary and perhaps a great deal more than practically feasible.

Expressions for the overall lost availability rate per kilogram of vehicle mass (i.e. the entropy generation rate per kilogram of vehicle mass) for a vehicle in accelerating, climbing flight in the atmosphere are derived. It is shown that the overall lost availability rate can be found by the superposition of the separate lost availability rates associated with 1) vehicle climb in drag-free nonaccelerating flight, 2) vehicle acceleration in drag-free nonclimbing flight, and 3) vehicle flight in nonaccelerating, nonclimbing flight. Complementary expressions for the overall lost availability rate per square meter of frontal vehicle (cross-sectional) area are derived in terms of losses associated with the propulsion system and losses associated with the external drag. These expressions are cast in terms of engine specific impulse ratings, propellant heating values, and flight characteristics such as drag coefficient.

Using these methods, simple configurations representing H_2-O_2 rocket-powered vehicles and H_2–air air-breathing vehicles at 30 km altitude are then analyzed. The rocket-powered configuration exhibits a distinct minimum-loss flight velocity for a given altitude; this minimum-loss velocity for the general case is obtained analytically. When contours of lost availability rate are plotted versus velocities and ranges that span the access-to-space range, the rocket configuration exhibits intriguing regions of low-loss rates within the velocity-altitude space; specifically a low-lost rate corridor exists which bridges sea level launch to a flight velocity of approximately 4500 m/s; a distinct low-loss rate column (or zone in the velocity-altitude space) then exists above this limit. This low-loss rate column approximately spans flight velocities of 4000 to 5000 m/s and ranges across altitudes from 50 km to orbital altitudes (for the specifics of the configuration examined). It is interesting to envision the use of such information (especially when combined with time-integration of resultant losses across entire missions) to assist in the optimization of rocket-powered vehicles and missions.

Similar results are obtained for an air-breathing configuration in terms of analyzing lost availability characteristics. For this case there is a distinct region of high loss associated with high-velocity, low altitude flight that an air-breathing vehicle must essentially skim due to thrust and drag power considerations (and resultant low accelerations) and in order to provide adequate lift generation and operability margins.

The techniques developed in this work provide the basic theoretical and analytical framework necessary for the thermodynamically consistent examination of aerospace vehicle performance. This is done from the standpoint of the overall general availability balance which governs flight vehicles. Availability analysis, in principle, allows the single-metric analysis of losses across all subsystems and processes within an aerospace system or mission; this capability should prove useful in the analysis, design and optimization of aerospace vehicles and missions.

Acknowledgments

The authors would like to thank the Air Force Office of Scientific Research for partial support for this work during the summer of 2007, 2008, and 2009, as well as Thomas Curran for his long-standing and continual support of fundamental analytical work in the area of availability.

References

[1] Bejan, A., "Entropy Generation and Exergy Destruction," *Entropy Generation Minimization: The Method of Thermodynamic Optimization of Finite-Size Systems and Finite-Time Processes*, CRC Press, New York, 1996, pp. 21–42.

[2] Moorhouse, D., "Introduction: Exergy," *Journal of Aircraft*, Vol. 40, No. 1, 2003, p. 10. doi:10.2514/2.3087

[3] Oswatitsch, K., "General Equations and Theorems," *Gas Dynamics*, Academic Press, New York, 1956, pp. 177–210.

[4] Giles, M. and Cummings, R., "Wake Integration for Three-Dimensional Flowfield Computations: Theoretical Development," *Journal of Aircraft*, Vol. 36, No. 2, 1999, pp. 357–365. doi:10.2514/2.2465

[5] Hunt, D., Giles, M., and Cummings, R., "Wake Integration for Three-Dimensional Flowfield Computations: Applications," *Journal of Aircraft*, Vol. 36, No. 2, 1999, pp. 366–373. doi:10.2514/2.2466

[6] Riggins, D. W., Taylor, T., and Moorhouse, D., "Methodology for Performance Analysis of Aerospace Vehicles Using the Laws of Thermodynamics," *Journal of Aircraft*, Vol. 43, No. 4, 2006, pp. 953–963.
doi:10.2514/1.16426

[7] Foa, J., "Efficiencies: Propulsive Cycles," *Elements of Flight Propulsion*, Wiley, New York, 1960, pp. 274–287.

[8] Builder, C. H., "On the Thermodynamic Spectrum of Air-Breathing Propulsion," AIAA Paper 64-243, June 1964.

[9] Riggins, D. W., "The Thermodynamic Continuum of Jet Engine Performance; The Principle of Lost Work due to Irreversibility in Aerospace Systems," *International Journal of Thermodynamics*, Vol. 6, No. 3, 2003, pp. 107–120.

[10] Lewis, J. H., "Propulsive Efficiency from an Energy Utilization Standpoint," *Journal of Aircraft*, Vol. 13, No. 4, 1976, pp. 299–302.
doi:10.2514/3.44525

[11] Curran, T. and Craig, R., "The Use of Stream Thrust Concepts for the Approximate Evaluation of Hypersonic Ramjet Engine Performance," USAF Aero-Propulsion Lab. TR-73-38, 1978.

[12] Riggins, D., McClinton, C. R., and Vitt, P., "Thrust Losses in Hypersonic Engines Part 1: Methodology," *Journal of Propulsion and Power*, Vol. 13, No. 2, 1997, pp. 281–287.
doi:10.2514/2.5160

[13] Riggins, D., "Thrust Losses in Hypersonic Engines Part 2: Applications," *Journal of Propulsion and Power*, Vol. 13, No. 2, 1997, pp. 288–295.
doi:10.2514/2.5161

[14] Roth, B., "Comparison of Thermodynamic Loss Models Suitable for Gas Turbine Propulsion," *Journal of Propulsion and Power*, Vol. 17, No. 2, 2001, pp. 324–332.
doi:10.2514/2.5745

[15] Roth, B., "A Work Potential Perspective of Engine Component Performance," *Journal of Propulsion and Power*, Vol. 18, No. 6, 2002, pp. 1183–1190.
doi:10.2514/2.6077

[16] Clarke, J., and Horlock, J., "Availability and Propulsion," *Journal of Mechanical Engineering Science*, Vol. 17, No. 4, 1975, pp. 223–232.
doi:10.1243/JMES_JOUR_1975_017_033_02

[17] Czysz, P. and Murthy, S., "Energy Analysis of High-Speed Flight Systems," *High-Speed Flight Propulsion Systems*, edited by T. Curran and S. Murthy, Progress in Astronautics and Aeronautics, Vol. 137, AIAA, Washington, D.C., 1991, pp. 143–236.

[18] Riggins, D., "Evaluation of Performance Loss Methods for High-Speed Engines and Engine Components," *Journal of Propulsion and Power*, Vol. 13, No. 2, 1997, pp. 296–304.
doi:10.2514/2.5162

[19] Riggins, D., "High-Speed Engine/Component Performance Assessment Using Exergy and Thrust-Based Methods," NASA CR-198271, Jan. 1996.

[20] Greene, G., "An Entropy Method for Induced Drag Minimization," SAE Paper 892344, Sep. 1989.

[21] Roth, B., "Aerodynamic Drag Loss Chargeability and its Implications in the Vehicle Design Process," AIAA Paper 2001-5236, Oct. 2001.

[22] Roth, B. and Mavris, D., "A Generalized Model for Vehicle Thermodynamic Loss Management and Technology Concept Evaluation," AIAA Paper 2000-5562, Oct. 2000.

[23] Riggins, D., Camberos, J., and Baker, M., "Analysis of Power Losses and Wake Entropy Production for Hypersonic Flight Vehicles," AIAA Paper 2006-7904, Nov. 2006.